

RSC Advances



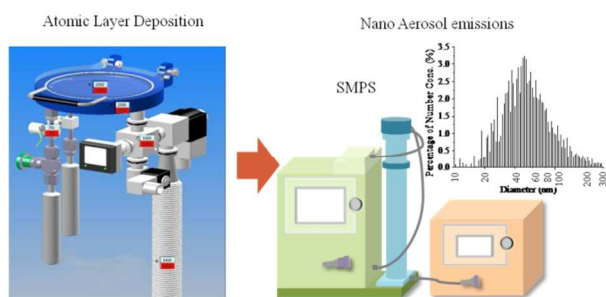
This is an *Accepted Manuscript*, which has been through the Royal Society of Chemistry peer review process and has been accepted for publication.

Accepted Manuscripts are published online shortly after acceptance, before technical editing, formatting and proof reading. Using this free service, authors can make their results available to the community, in citable form, before we publish the edited article. This *Accepted Manuscript* will be replaced by the edited, formatted and paginated article as soon as this is available.

You can find more information about *Accepted Manuscripts* in the [Information for Authors](#).

Please note that technical editing may introduce minor changes to the text and/or graphics, which may alter content. The journal's standard [Terms & Conditions](#) and the [Ethical guidelines](#) still apply. In no event shall the Royal Society of Chemistry be held responsible for any errors or omissions in this *Accepted Manuscript* or any consequences arising from the use of any information it contains.

Table of Contents Entry



The ALD process emissions and the associated chemical reaction mechanism inside the ALD of Al_2O_3 system are studied and reported.

Atomic Layer Deposition of Al₂O₃ Process Emissions

Cite this: DOI: 10.1039/x0xx00000x

Lulu Ma, Dongqing Pan, Yuanyuan Xie and Chris Yuan*

Received 00th January 2012,
Accepted 00th January 2012

DOI: 10.1039/x0xx00000x

www.rsc.org/

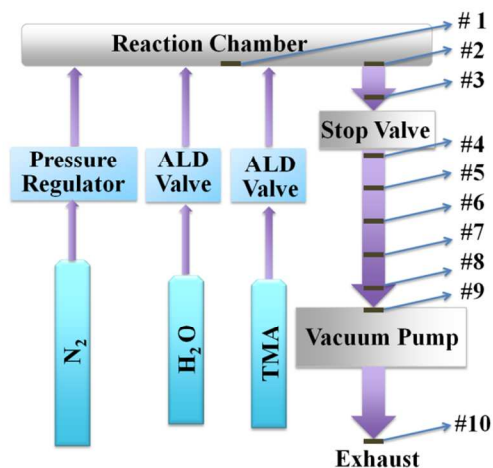
The ALD process emissions and the associated chemical reaction mechanism inside the ALD of Al₂O₃ system are studied and reported. In gaseous emissions, 3.33 Vol.% of CH₄ and 6.45×10⁻² Vol.% of C₂H₆ are found. Net peak emissions of aerosols are found between 1×10³ and 1×10⁴ #/cm³ and net total emissions of 25 cycles are in the range of 6.0×10⁵ and 2.5×10⁶ particles. Most aerosols are determined as ultrafine particles with diameter smaller than 100 nm. Purging time has significant impacts on emission concentrations but no effect on size distribution. Both main and side chemical reactions are observed in the ALD system. X-ray photoelectron spectroscopy (XPS) shows that besides O-Al which represents the existence of Al₂O₃, significant amount of C-containing by-products are also generated. Chemical bonds observed in C-containing resultants are C-H, C-O and C=O. Main reactions can be considered stable to a certain extent, while side reactions accelerate along internal tubes and finally exceed the speed of main reactions near the outlet of the ALD system. These results could help understand the potential environmental impacts of ALD nanotechnology and guide the technology's sustainable scale-up in future.

- 1 **Introduction** 18
 2 In recent years, Atomic layer deposition (ALD) has found 20
 3 broad array of industrial applications including 21
 4 semiconductors,^{1,2} solar cells,^{3,4} polymers,^{5,6} and catalyst.⁷ 22
 5 nature, ALD operates by alternating exposure of a substrate 23
 6 two or more precursors in a cyclic manner. Advantages of ALD 24
 7 include: 1) thickness of ALD film can be controlled at atom 25
 8 scale; 2) deposition can be made on complex surfaces; 26
 9 uniform, conformal and pinhole-free nano-scale thin films can 27
 10 be fabricated. ALD technology can be used to deposit a wide 28
 11 variety of materials. Usually ALD of Al₂O₃ is studied as the 29
 12 model process of ALD technology. In this process, Al₂O₃ thin 30
 13 film is usually obtained through a binary reaction of H₂O and 31
 14 Trimethylaluminum (TMA) with a typical growth rate of 1 32
 15 per cycle.⁸ The overall reaction in ALD of Al₂O₃ can be 33
 16 described as: 34
 17 2Al(CH₃)₃+3H₂O→Al₂O₃+6CH₄ ΔH=-376kcal 35
- ALD is a self-limited process and only a small portion of the precursors loaded into ALD chamber is deposited on the substrate, while a large portion is discarded as wastes and emissions.⁹ Past ALD research was focused on ALD technology development. There are few researches on ALD process emissions and its relevant environmental impacts. As per the reaction mechanism in ALD process, theoretical emissions are TMA, Al₂O₃, CH₄ and some intermediate reactants. Once released into atmosphere, they can generate certain environmental impacts and also pose potential risks of exposure to both occupational and public health. For instance, CH₄ is a flammable and a major greenhouse gas.¹⁰ Global warming potential of CH₄ is 25 times higher than that of CO₂, so it has a much larger greenhouse effect.¹¹ Intake of Al₂O₃ through human exposure could cause a series of neuro-toxicity diseases, including reduction of memory, impairment of psychomotor reaction and disorder of emotional balance.¹² As a nano-manufacturing process, ALD of Al₂O₃ also produces

1 significant amount of aerosol emissions. Aerosols with high
 2 concentrations can cause adverse effects on human health. It
 3 well known that particles smaller than 10 μm are able
 4 penetrate alveolar region of lung. Ultrafine particles, small
 5 than 100 nm, can penetrate membranes of respiratory system
 6 enter blood and finally arrive in brain through circulatory
 7 system.^{12,13} While the ALD of Al_2O_3 process emissions are
 8 grave concerns because of their potential adverse effects on the
 9 environment and human health, however, there is no scientific
 10 study so far conducting on the process emissions and the behavior
 11 mechanism from ALD nano-manufacturing process. This paper
 12 is to report our experimental results on the ALD process
 13 emissions and the findings on the associated chemical reaction
 14 mechanism. The results may facilitate understanding of the
 15 potential environmental impacts of the ALD nanotechnology
 16 and guide its sustainable scale-up for future large-scale
 17 industrial applications.

18 Experimental Methods

19 Instrumental Setup and Sample Collection



20
 21 Figure 1. Schematic of Al_2O_3 ALD system (Savannah 100,
 22 Cambridge Nano Tech Inc.).

23 Figure 1 is a schematic of the ALD system (Savannah 100,
 24 Cambridge Nano Tech Inc.). Two precursors: H_2O (ultrapure
 25 grade) and trimethylaluminum (TMA, Strem Chemicals Inc.)
 26 were exposed into the reaction chamber alternatively,
 27 controlled by two individual diaphragm ALD valves
 28 (Swagelok). ALD reactions are performed in cycles. One cycle
 29 of ALD reaction has four basic steps: (1) pulse H_2O into
 30 reaction chamber; (2) purge the chamber to remove extra H_2O ;
 31 (3) pulse TMA into reaction chamber; (4) purge the chamber to
 32 remove extra TMA. TMA is an extremely flammable chemical
 33 and will ignite spontaneously when come in contact with air.
 34 Therefore, exposure of TMA in air must be avoided.¹⁴ In
 35 experimental tests, exposure time of both H_2O and TMA was
 36 fixed at 0.015 s and purging time was set in the range between
 37 4 and 20 s. 20 sccm of N_2 was used as carrier gas to flow
 38 through the system constantly. A stop valve was installed below

the reaction chamber to help control gas flow. Stop valve and
 ALD valves were operated by compressed air. An inner disk
 heater embedded in the reaction chamber and heating jackets
 for other components were used to provide appropriate
 temperature to the system. In this study, temperature inside the
 reaction chamber was set at 200 $^\circ\text{C}$. ALD valves and exhaust
 system including stop valve and pipeline were heated to 150
 $^\circ\text{C}$. Neither TMA nor H_2O needed to be heated; so cylinders of
 two precursors were placed in room temperature. A vacuum
 pump (XDS 10, Edwards Vacuum, Inc.) was installed at the
 end of the exhaust pipeline to provide a low pressure (about 0.4
 torr) to the whole system and pump out the extra precursors
 from the chamber.

The ALD process emissions and the emission generation
 mechanism are systematically investigated along the exhaust
 pipeline of the ALD system. 10 pieces of Si wafers are prepared
 as sample holders to collect chemical resultants within the ALD
 exhaust pipeline. Their locations are labeled in the schematic of
 instrumental setup in figure 1. Sample 1 locates in the center of
 the reaction chamber. Sample 2 and 3 are placed in the exhaust
 pipeline above the stop valve, and sample 4-9 are placed below
 the stop valve. Sample 10 is placed at the pump outlet under
 ambient temperature. Purging time between two pulses was set
 at 8 s. In this study, these silicon samples are exposed to the
 same ALD process reactions. In order to improve the efficiency
 of particle collection, particles emitted from vacuum pump are
 also collected on a piece of TEM grid (TED PELLA, INC.,
 Prod No. 01824) by aerosols sampler (TSI 3089), where
 charged particles deposited on a piece of conductive grid
 through electric field.

69 Emission Analysis

70 Aerosols emitted from ALD reaction were measured directly at
 71 outlet of pump without pre-treatment. Concentration of aerosols
 72 was measured by ultrafine condensation particle counter
 73 (UCPC, TSI 3776). Size distribution was obtained using a
 74 scanning mobility particle sizer (SMPS, TSI 3936) which
 75 consists of an electrostatic classifier (TSI 3080) and UCPC.
 76 Detailed instrument setup is described in supporting
 77 information. In this experiment, five different purging times
 78 were used at 4s, 8s, 12s, 16s and 20 s to study their effects on
 79 the ALD process emissions.

Gas emissions were collected at the outlet of pump by a sealed
 Swagelok gas cylinder and analyzed in the ORS lab (Oneida
 Research Services Inc.). Purging time between pulses was set at
 8 s, the same as Si wafer analysis.

Analysis of Chemicals Deposited on Si Wafer

Because Si wafer was not transparent, reflection method was
 selected for UV-Vis spectroscopy measurement (light source:
 DT 1000CE, Analytical Instrument Systems, Inc.; detector:
 SD2000, Ocean Optics, Inc.). A piece of clean Si wafer was
 used as background and its reflection was set at 100 %.
 X-ray photoelectron spectroscopy (XPS, HP 5950A ESCA
 Spectrometer) was used to determine functional groups of

1 depositions. Concentration of each element was provided by
 2 energy-dispersive X-ray spectroscopy (EDS, QUANTAX EDS,
 3 Bruker Corp.).

4 Results and Discussion

5 Gaseous Emissions

6 Analysis of the gaseous emissions shows the existence of N₂,
 7 CH₄, H₂O and C₂H₆. Concentration of each component is listed
 8 in table 1.

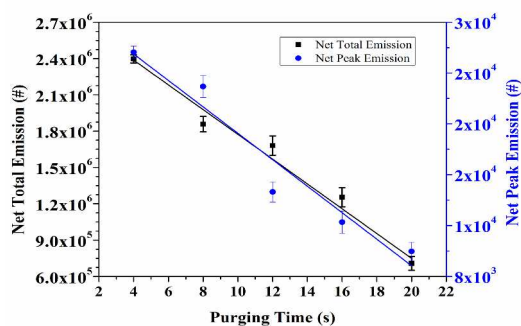
9 Table 1 Concentrations of Each Component in Gaseous Emission.

Component	Concentration inALD Emission(Vol.%)
N ₂	94.61
CH ₄	3.22
H ₂ O	1.99
C ₂ H ₆	6.45×10 ⁻²

10 N₂ has the highest concentration at 94.98 Vol.% because it is
 11 used as carrier gas to flow through the system consistently. The
 12 ALD system is airtight. Though compressed air is used to
 13 operate stop valve and ALD valves, it is not introduced into the
 14 system. Both N₂ and compressed air are in dry grade, so 1.86
 15 Vol.% of H₂O is from extra H₂O precursor only. CH₄, the
 16 theoretical gaseous resultant, has concentration of 3.10 Vol.%,
 17 which is close to the lower good flammability limit of CH₄ at
 18 Vol.%.¹⁵ 6.01×10⁻² Vol.% of C₂H₆ is also found in the gaseous
 19 emission. In the ALD reaction of TMA and H₂O, a small
 20 amount of Al-Al is commonly observed in XPS data. This peak
 21 is ably reduced by replacing H₂O with O₃.¹⁶ Methyl radicals
 22 CH₃• can be generated by reacting TMA with Al.¹⁷ They are
 23 highly reactive and form C₂H₆ easily.

24 Aerosol Emissions

25 Aerosols emissions from the ALD of Al₂O₃ reactions, including
 26 net peak emission and net total emissions of 25 cycles, are
 27 shown in figure 2.



28
 29 Figure 2. Net peak emissions of aerosols and net total emission of
 30 cycles of ALD reaction measured at pump outlet.

31

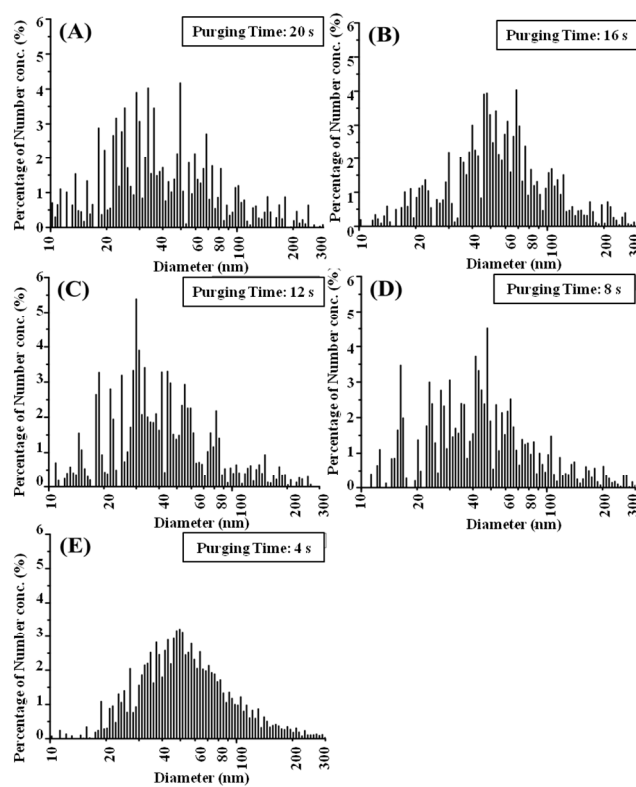
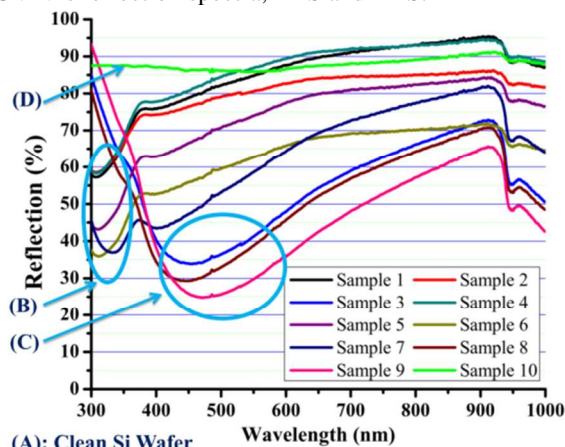


Figure 3. (A), (B), (C), (D) and (E) are results of size distribution of aerosols emitted at 5 different purging times: 4, 8, 12, 16 and 20 s, respectively.

32
 33 Net peak emission of aerosols is in the range of 1.0×10^4 and
 34 2.6×10^4 #/cm³. The emission decreases with the increase of
 35 purging time. Average global aerosol concentration at
 36 continental boundary layer was detected in the range of 1×10^3
 37 to 1×10^4 #/cm³.¹⁸ So concentration of aerosols emitted by ALD
 38 reaction is 3 to 10 times larger than the average concentration
 39 of global aerosols, and thus is a significant source of air
 40 pollution. Concentration of net total emissions is in the range of
 41 6.0×10^5 and 2.5×10^6 particles. Net total emissions also decrease
 42 with the increase of purging time. Since pulsing time of each
 43 precursor is fixed at 0.015 s, the amounts of precursors injected
 44 into the reaction chamber per cycle are the same. The drop of
 45 total emission at large purging time indicates that more
 46 precursors are adsorbed in the ALD pipeline. Once deposited
 47 by precipitation, the surface of pipeline will have a larger
 48 tendency of further deposition.¹⁹ These precipitations
 49 accumulated along ALD pipeline will lower the heat transfer,
 50 prevent gas flow and decrease energy efficiency.^{19,20}
 51 Though purging time shows a great influence on the number
 52 concentration of aerosol emission, it has limited effect on size
 53 distribution, as shown in figure 3. Size distribution of aerosols
 54 locates in the range between 10 and 300 nm regardless of
 55 purging times varying from 4 to 20s. Most aerosols are ultrafine
 56 particles smaller than 100 nm.

60 UV-Vis Analysis of Chemicals Deposited on Si Wafer

1 To identify the side reactions in the ALD system and identify
 2 the emission mechanism from ALD of Al_2O_3 process,
 3 components and chemical properties of ALD emissions and the
 4 samples installed along internal pipeline are investigated using
 5 UV-Vis reflection spectra, XPS and EDS.

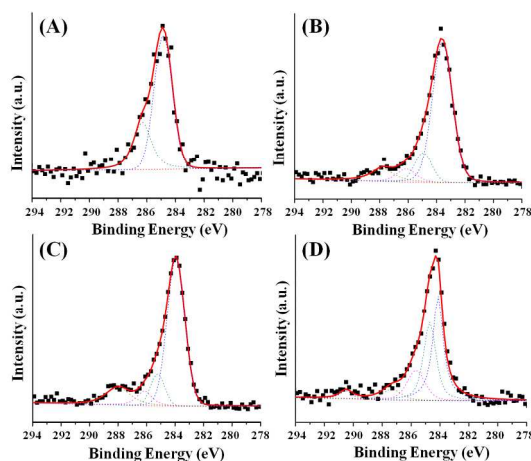


6 (A): Clean Si Wafer

7 Figure 4. UV-Vis spectra of the 10 samples inside ALD system.

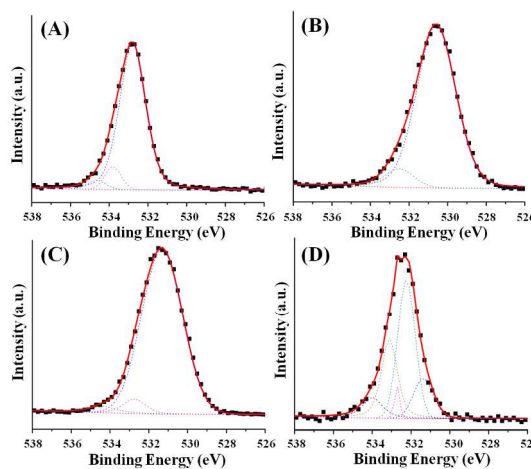
8 Figure 4 is the UV-Vis reflection spectra of the 10 samples
 9 between 300 and 1000 nm. A piece of clean Si wafer is used as
 10 background and its reflection is set at 100%. By defining clean
 11 Si piece having the first type of UV-Vis spectrum (A), the
 12 spectra of the 10 samples can be divided into 3 types: (B), (C)
 13 and (D). Type (B), having the smallest reflection at about 350
 14 nm, is observed on sample 1, 2, 4, 5 and 6. Type (C), showing
 15 smallest reflection at about 450 nm, is found on sample 3, 8 and
 16 9. (D) is the result of sample #10 collected on the outlet of
 17 pump. The optical bandgap of ALD Al_2O_3 film is determined at
 18 6.4 ± 0.1 eV, so it is transparent above 200 nm.^{21,22} However,
 19 all of the samples in figure 4 show significant reflection drop,
 20 indicating that chemicals other than Al_2O_3 have been generated
 21 and emitted into atmosphere. Reflection curves of sample 1, 2,
 22 4, 5, and 6 decrease gradually from sample 1 to 2 and 4 to 6,
 23 respectively with similar spectrum shape. Continuous reflection
 24 drop indicates increase of film thickness on Si wafer. Sample 4
 25 is the first sample below the stop valve. Because there is no
 26 instrumental component impeding the flow between sample 4
 27 and 9, gas flow is more stable in this region than in the pipeline
 28 above stop valve. The shape of reflection curves starts to
 29 change from sample 7 and become stable at 8 and 9. Sample 8
 30 is installed above the stop valve but has a similar spectrum as
 31 and 9. Reason of this phenomenon is due to the disruption of
 32 the stop valve between the sample 3 and 4. Precursors are
 33 retarded by it and thus react for a longer time. The change of
 34 spectrum curve observed on sample 3, 8 and 9 indicates
 35 generation of chemicals that are different from those observed
 36 on (B). Sample #10, collected at the outlet of pump, has much
 37 higher reflection. Therefore, the amount of emissions of ALD
 38 reaction is limited, and most of resultants are adsorbed on the
 39 inner wall of the system as precipitations.

40 XPS Analysis of Chemicals Deposited on Si Wafer

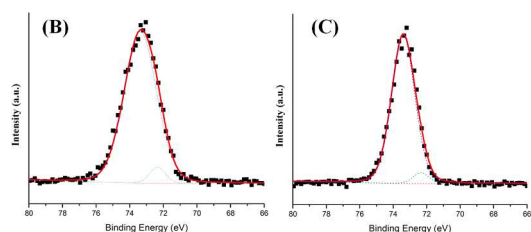


41

42 Figure 5. XPS data of Carbon. (A), (B), (C) and (D) are correlated
 43 with the four types mentioned in figure 4.



44 Figure 6. XPS data of Oxygen. (A), (B), (C) and (D) are correlated
 45 with the four types mentioned in figure 4.



46 Figure 7. XPS data of Al. (B) and (C) are correlated with the two
 47 types mentioned in figure 4.

48 Chemical compositions of the four groups of samples are
 49 measured by XPS. XPS spectra between 0 and 900 eV is shown
 50 in figure S2 in the Supporting Information. Figure 5 and 6
 51 illustrate detailed C and O spectra, respectively. (A), (B), (C)
 52 and (D) are the four types of samples mentioned in figure 4.
 53 Peaks of C in (B), (C) and (D) are about 3 to 4 times higher
 54 compared with that of (A), indicating that significant amounts
 55 of C-containing by-products have been generated by ALD
 56 reaction. C in (B) exists in the form of C-C/C-H (283.2 eV), C-
 57 O (284.8 eV) and C=O (287.2). Meanwhile, three peaks are
 58 found in the peak of O: Al-O (530.1 eV), C-O (531.3 eV) and
 59 C=O (532.5 eV). Sample (C) also contains C-C/C-H (283.5

1 eV), C-O (285.0 eV) and C=O (287.6 eV) in the peak of C and
 2 Al-O (530.3 eV), C-O (531.4 eV) and C=O (532.4 eV) in the
 3 peak of O. However, relative intensity of C-O and C=O in (B)
 4 are higher than that in (B). Four peaks of C are observed
 5 sample (D): C-C/C-H (283.6 eV), C-O (285.3 eV), C=O (287.58
 6 eV) and C-F (290.0 eV), where C-F is exhausted by Teflon
 7 membrane inside Edwards XDS 10 pump. O in sample (D)
 8 found containing Si-O-Si (531.3 eV), C=O (531.8 eV), Si-O
 9 (532.3 eV) and C-O (533.1 eV).²³ Al deposits on the type
 10 and (C) is found as Al-O and Al-Al. The results of Al collected
 11 on sample (B) and (C) are shown in figure 7. A small amount
 12 Al-Al is commonly observed in the reaction of TMA and H₂O
 13 and can be reduced by replacing H₂O with O₃.^{16,24} Because
 14 efficiency of aerosol collection on Si wafer is limited and
 15 density of aerosol distribution is relatively small, no Al
 16 observed on sample (D) by XPS.
 17 Neither H₂O nor N₂ contains C, so TMA is the only source
 18 C. Decomposition of TMA on Si (100) wafer has been
 19 observed incompletely.²⁵ Since the peak of C-Al is not
 20 detected, all the TMA has participated in either main or side
 21 reactions.^{26,27} Reactions of TMA and -OH are able to generate
 22 intermediate reactants (-O)(-OH)Al(CH₃)₂ and (-O)(-
 23 OH)Al(CH₃).^{28,29} O-O bond is not stable and alkyl peroxide has
 24 been found decomposable into ketone and alcohol.³⁰ Besides
 25 generating C₂H₆, CH₃• can react with ROR and generate C₂H₅
 26 and ROR•, where R represents alkyl groups.³¹ These radicals
 27 can contribute to the formation of C-containing by-products.
 28 Since no gas with m/z above 45 is observed, C-O, C=O and
 29 H containing chemicals are all emitted as aerosols at outlet
 30 the pump.

31 EDS Analysis of Chemicals Deposited on Si Wafer

32 Measurements of atomic concentration of the 10 samples are
 33 also accomplished by EDS. The results are listed in table S1 in
 34 the Supporting Information. Among these 10 samples, samples
 35 4 to 9 locate in a relatively stable region. Sample 4 has higher
 36 concentration of carbon but its UV-Vis spectrum and XPS data
 37 are similar with other samples in type (B). This phenomenon is
 38 due to the stop valve installed between sample 3 and 4. C is
 39 detected on all the samples, indicating that side reactions are
 40 found all over the system. Concentration of Al from sample 5 to
 41 9 does not change significantly, while concentrations of C and
 42 O both increase gradually. Therefore, reaction that generates
 43 Al₂O₃ is stable to a certain extent, while side reactions that
 44 generate C-containing chemicals accelerate along the pipeline.
 45 At the lower part of system, where sample 8 and 9 are placed,
 46 there are more C-containing chemicals generated than Al-
 47 containing chemicals. EDS measured on particles collected on
 48 TEM grid shows that 4.40±1.00% of Al, 3.31±1.07% of C,
 49 83.46±16.11% of Cu, 4.96±0.96% of F and 3.86±0.74% of O
 50 are containing in emitted particles.

51 Conclusions

52 Both gaseous emissions and aerosols from ALD of Al₂O₃
 53 process are investigated and reported. In the measurement of

gaseous emission, CH₄ and C₂H₆ are found generated by ALD
 reactions, where CH₄ is the second concentrated component in
 the gaseous emission. Large amounts of aerosols that are 3 to
 10 times more concentrated than average global aerosols are
 generated. Most of them are in the ultrafine range with diameter
 smaller than 100 nm. Purging time has no effects on aerosol
 size distribution, but significantly impacts the total net emission
 of aerosols. In a longer purging time, more aerosols are
 adsorbed on system pipeline as precipitation. Series
 measurements of samples collected along ALD exhaust system
 reflected the emission generation mechanism from both main
 and side chemical reactions. Aerosols emitted from the ALD
 reactions have both Al-containing and C-containing
 compounds, where C-containing compounds are generated
 through side reactions. XPS shows that chemical bonds,
 including C-H, C-O and C=O, are contained in by-products.
 The main reactions can be considered stable to a certain extent,
 while side reactions accelerate and exceed the speed of main
 reactions at the last three samples.

Acknowledgements

This research is supported by National Science Foundation
 (CMMI-1200940). The author would also like to thank
 Jianyang Li, Xianfeng Gao and Dongsheng Guan for their
 assistance in the experiments.

Notes and references

*Department of Mechanical Engineering, University of Wisconsin
 Milwaukee, Milwaukee 53211, USA. E-mail: Cyuan@uwm.edu; Tel: +1-
 414-229-5639

† Electronic Supplementary Information (ESI) available: [details of any
 supplementary information available should be included here]. See
 DOI: 10.1039/b000000x/

- 1 M. Huang, Y. Chang, C. Chang, Y. Lee, P. Chang, J. Kwo, T. Wu
 and M. Hong, *Appl. Phys. Lett.*, 2005, **87**, 252104.
- 2 P. Ye, B. Yang, K. Ng, J. Bude, G. Wilk, S. Halder and J. Hwang,
Appl. Phys. Lett., 2005, **86**, 063501.
- 3 X. Gao, J. Chen and C. Yuan, *J. Power Sources*, 2013, **240**, 503-
 509.
- 4 X. Gao, D. Guan, J. Huo, J. Chen, and C. Yuan, *Nanoscale*, 2013,
5, 10438-10446.
- 5 S. George, *Chem. Rev.*, 2010, **110**, 111-131.

- 6 E. Langereis, M. Creatore, S. Heil, M. van de Sanden and W. Kessels, *Appl. Phys. Lett.*, 2006, **89**, 081915.
- 7 M. Pellin, P. Stair, G. Xiong, J. Elam, J. Birrell, L. Curtiss, S. George, C. Han, L. Iton, H. Kung, M. Kung and H. Wang, *Catal. Lett.*, 2005, **102**, 127-130.
- 8 J. Koo, S. Kim, S. Jeon and H. Jeon, *J. Korean Phys. Soc.*, 2006, **48**, 131-136.
- 9 J. Huo, X. Lin and C. Yuan, *Proceedings of 2012 ASME Manufacturing Science and Engineering Conference*, Notre Dame, Indiana, USA, June 4-8, 2012.
- 10 D. Lashof and D. Ahuja, *D. R. Nature*, 1990, **344**, 529-531.
- 11 P. Forster, V. Ramaswamy, P. Artaxo, T. Bernsten, R. Betts, D. Fahey, J. Haywood, J. Lean, D. Lowe, G. Myhre, J. Nganga, R. Prinn, G. Raga, M. Schulz and R. Van Dorland, Changes in Atmospheric Constituents and in Radiative Forcing. In *Climate Change 2007: The Physical Science Basis. Contribution of Working Group I to the Fourth Assessment Report of the Intergovernmental Panel on Climate Change*; S. Solomon, D. Qin, M. Manning, Z. Chen, M. Marquis, K. Averyt, M. Tignor, H. Miller, H., eds; Cambridge University Press: Cambridge, United Kingdom and New York, NY, USA, 2007; pp 210-216.
- 12 D. Krewski, R. Yokel, E. Nieboer, D. Borchelt, J. Cohen, J. Harry, S. Kacew, J. Lindsay, A. Mahfouz, and V. Rondeau, *J. Toxicol. Environ. Health B Crit Rev.*, 2007, **10**, 1-269.
- 13 U. Pöschl, *Angew. Chem. Int. Ed.*, 2005, **44**, 7520-7540.
- 14 *Trimethylaluminum*; MSDS No. 98-4003; Strem Chemicals, Inc: Newburyport, MA, April 21, 2011.
- 15 K. Cashdollar, I. Zlochower, G. Greena, R. Thomas, and M. Hertzberg, *J. LOSS PREVENT PROC*, 2000, **13**, 327-340.
- 16 J. Kim, D. Kwon, K. Chakrabarti, C. Lee, K. Oh and J. Lee, *J. Appl. Phys.*, 2002, **92**, 6739.
- 17 D. Squire, C. Dulcey and M. Lin, *J. Vac. Sci. Technol. B*, 1985, **3**, 1513.
- 18 D. Spracklen, K. Carslaw, J. Merikanto, G. Mann, C. Reddington, S. Pickering, J. Ogren, E. Andrews, U. Baltensperger, E. Weingartner, M. Boy, M. Kulmala, L. Laakso, H. Lihavainen, N. Kivekäs, M. Komppula, N. Mihalopoulos, G. Kouvarakis, S. Jennings, C. O'Dowd, W. Birmili, A. Wiedensohler, R. Weller, J. Gras, P. Laj, K. Sellegri, B. Bonn, R. Krejci, A. Laaksonen, A. Hamed, A. Minikin, R. Harrison, R. Talbot, and J. Sun, *Atmos. Chem. Phys.*, 2010, **10**, 4775-4793.
- 19 K. Hyllestad, Scaling of Calcium Carbonate on a Heated Surface in a Flow Through System with Mono Ethylene Glycol. M.S. Thesis, Norwegian University of Science and Technology, Trondheim, Norway, 2008.
- 20 M. Crabtree, D. Eslinger, P. Fletcher, M. Miller, A. Johnson and G. King, *Oilfield Rev.*, 1999, **11**, 30-45.
- 21 G. Dingemans and W. Kessels, *J. Vac. Sci. Technol. A*, 2012, **30**, 040802.
- 22 G. López, P. Ortega, C. Voz, I. Martín, M. Colina, A. Morales, A. Orpella and R. Alcubilla, *Beilstein J. Nanotechnol.*, 2013, **4**, 726-731.
- 23 A. Namiki, K. Tanimoto, T. Nakamura, N. Ohtake and T. Suzuki, *Surface Science*, 1989, **222**, 530-554.
- 24 T. Kubo, J. Freedman, Y. Iwata and T. Egawa, *Semicond. Sci. Technol.*, 2014, **29**, 045004.
- 25 T. Gow, R. Lin, L. Cadwell, F. Lee, A. Backman, and R. Masel, *Chem. Mater.*, 1989, **4**, 406-411.
- 26 M. Bou, J. Martin and Th. LeMogne, *Appl. Surf. Sci.* 1991, **47**, 149-161.
- 27 C. Hinnen, D. Imbert, J. Siffre, and P. Marcus, *Appl. Surf. Sci.*, 1994, **78**, 219-231.
- 28 A. Delabie, S. Sioncke, J. Rip, S. Elshocht, G. Pourtois, M. Mueller, B. Beckhoff and K. Pierloot, *J. Vac. Sci. Technol. A*, 2012, **30**, 01A127.
- 29 B. Gong and G. Parsons, *J. Mater. Chem.*, 2012, **22**, 15672.
- 30 N. Kornblum and H. DeLaMare, *J. Am. Chem. Soc.*, 1951, **73**, 880-881.
- 31 P. Gray, and A. Herod, *Trans. Faraday Soc.*, 1986, **64**, 2723-2734.